Vibrational properties of noble gas endohedral fullerenes
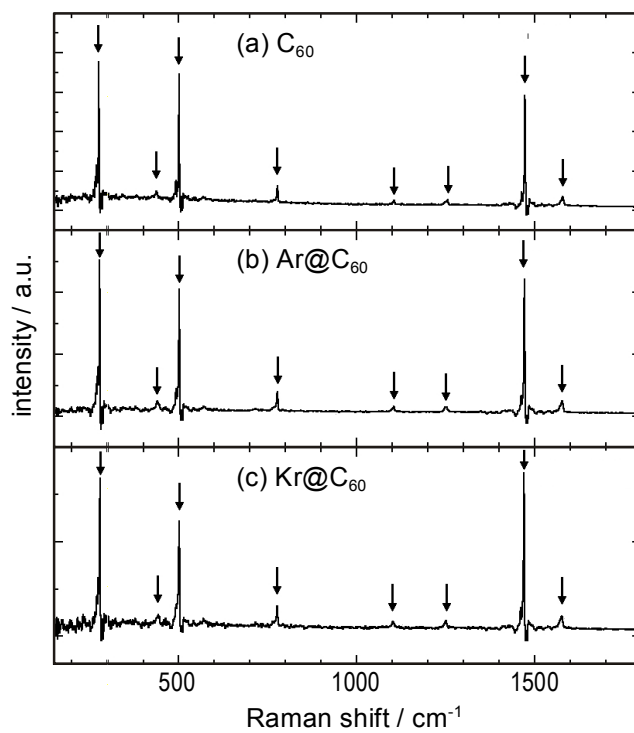
Electronic Supplementary Information

Figure 1. Raman spectra of (a)C_{60}, (b)Ar@C_{60} and (c)Kr@C_{60}. The vibration modes of C_{60} cage are indicated by arrows.
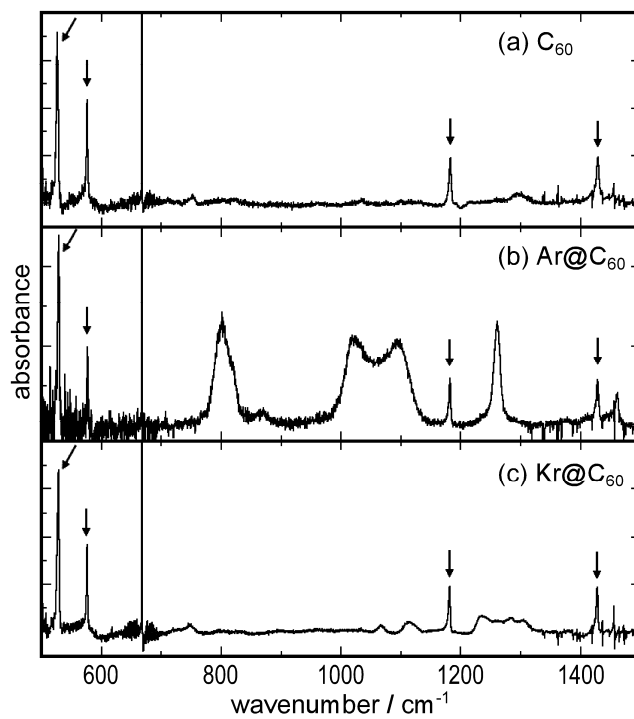
Figure 2. infrared spectra of (a)C_{60}, (b)Ar@C_{60} and (c)Kr@C_{60}. The vibrations of C_{60} cage are indicated by arrows.

A selective analysis of H_g vibration modes.

Without a full quantitative modeling, we will sketch the principle of treating the other modes in terms of spherical harmonics decomposition. As extrapolation, the shift pattern in H_g and T_{1u} will be understood as having the same causal roots, as function of radial vs. tangential movements, similarly to the A_g simpler case.

The radial components can be ascribed as the modulation of the radial A_g reference with symmetry adapted spherical harmonics:

$$q(l,\Gamma\alpha)_R = \sum_{i=1}^{60}\left(\sum_m \sigma_\alpha^{lm} Y_{lm}(\theta_i,\varphi_i)\right)\cdot\frac{d}{dR}\{x_i, y_i, z_i\} \quad . \tag{8}$$

The coefficients σ_α^{lm} are obtained from a Y_{lm} set the combination behaving as a given representation of the point group, namely H_g in our case. The index α is labeling the components of the given Γ representation. There are several procedures and conventions to derive symmetry adapted functions.[1] A convenient recipe for σ_α^{lm} values, circumventing the complicate algebra, is the corresponding selection among the eigenvectors of the following matrix:

$$T_{mk}^l = \sum_i Y_{lm}^*(\theta_i,\varphi_i)Y_{lk}(\theta_i,\varphi_i) \quad , \tag{9}$$

taken at each l case. The spherical functions evaluated at the θ_i, φ_i, polar coordinates of each atom in the cluster form the coefficient defining the amplitude and orientation of the local radial vector. The spherical harmonics were ascribed in their standard form, but in fact is convenient to work with the real definitions, converting the $Exp(\mathbf{i}m\varphi)$ factor in the Sine and Cosine components, $Y_{l|m|}^s$ and $Y_{l|m|}^c$. In a reasonable conceptual picture, the analytical description can be confined to the minimal set containing the desired three radial H_g components, namely $l = 2$, $l = 4$ and $l = 6$.

The modeling of the tangential H_g modes is more complex. We call here the apparatus of Tensor Surface Harmonics (TSH).[2,Error! Bookmark not defined.c] The TSH is a symmetry analysis apparatus, with applications in the electron structure[3] and vibrations[4] of clusters. The first order TSH, namely the vector surface harmonics, are defined as derivatives of spherical harmonics with respect of polar coordinates:

$$q(l,\Gamma\alpha)_V = \sum_{i=1}^{60}\sum_m \sigma_\alpha^{lm}\left[\left(\frac{\partial}{\partial\theta}Y_{lm}(\theta_i,\varphi_i)\right)\cdot\vec{\xi}(\theta_i,\varphi_i)+\left(\frac{\partial}{\partial\varphi}Y_{lm}(\theta_i,\varphi_i)\right)\cdot\vec{\zeta}(\theta_i,\varphi_i)\right] \tag{10.a}$$

$$\overline{q}(l,\Gamma\alpha)_{\overline{V}} = \sum_{i=1}^{60}\sum_m \overline{\sigma}_\alpha^{lm}\left[\left(\frac{\partial}{\partial\theta}Y_{lm}(\theta_i,\varphi_i)\right)\cdot\vec{\zeta}(\theta_i,\varphi_i)-\left(\frac{\partial}{\partial\varphi}Y_{lm}(\theta_i,\varphi_i)\right)\cdot\vec{\xi}(\theta_i,\varphi_i)\right] \quad , \tag{10.b}$$

where the tangential unit vectors are:

$$\vec{\xi}(\theta_i,\varphi_i) = \{\cos(\theta_i)\cos(\varphi_i), \cos(\theta_i)\sin(\varphi_i), -\sin(\theta_i)\} \tag{11.a}$$

$$\vec{\zeta}(\theta_i,\varphi_i) = \{-\sin(\varphi_i), \cos(\varphi_i), 0\} \quad . \tag{11.b}$$

The $q(l,\Gamma\alpha)_V$ functions are drawn from the so-called even vector harmonics, V_{lm}, possessing the same point group symmetries as the corresponding scalar Y_{lm} spherical harmonics. Qualitatively, the V_{lm}, vectors can be described as fluxes on the sphere surface, exiting from positive extremes and flowing toward negative minima of the Y_{lm} functions, having maximal amplitudes at the crossing of nodal borders. The functions denoted by $\overline{q}(l,\Gamma\alpha)_{\overline{V}}$ arise from companions called odd vector harmonics, $\overline{V}_{lm}$. In the case of I_h point group, their representations have reverted parity than the congener V_{lm} and Y_{lm} sets (namely H_u, instead of H_g). The pictorial description of V_{lm} suggests curl

vortices around the extremes points of the spherical harmonics, with different orientation, as function of the sign of Y_{lm} on the surface. The modes formed with even vector harmonics can be taken within the same count as the radial case, i.e. from the $l = 2$, $l = 4$ and $l = 6$ sets. The two remaining tangential modes can be considered as matched by odd vector harmonics. Due to reverted parity incorporated in the transformation, the H_g vibrations must be acquired from odd angular numbers, namely $l = 5$ and $l = 7$ (that match H_u in the Y_{lm} sets). Besides, the accurate description may require also ingredients from the second order TSH derivatives.

A different strategy to complete the H_g list with the last two components (instead of the $l = 5$ and $l = 7$ odd vector harmonics) is the modulation of tangential A_g mode with spherical harmonics (i.e. function of the τ parameter):
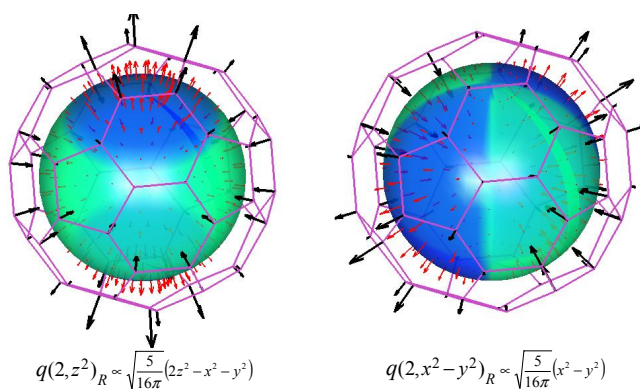
$$q(l,\alpha)_\tau = \sum_{i=1}^{60}\left(\sum_m \sigma_\alpha^{lm} Y_{lm}(x_i,y_i,z_i)\right)\cdot\frac{d}{d\tau}\{x_i,y_i,z_i\} . \tag{12}$$

By symmetry reasons, this kind of function can target the simulation of two tangential modes only, which is sufficient for our purpose. This is because the given coordinates should span the same representation as the edges in the icosahedron, which contains only two H_g components. These τ dependent functions can be regarded as a combination between first and higher orders in TSH expansion.

Due to difficulties in handling vector harmonics of higher order we confined here to the explicit use of simplest even vector harmonics set, $l = 2$, altogether with the above defined modulation of the tangential A_g movements. We do not aim the complete analytical decomposition, confining ourselves in checking the presence of the mentioned components.

The lowest H_g mode presents as about 73% radial $l = 2$ spherical harmonics and 26% even $l = 2$ vector harmonics, as illustrated in Figure 3. The second H_g mode is almost completely spanned by the radial $l = 4$ component (see Figure 4). The third H_g consists in 78% radial $l = 6$ function. Noticeably, the fourth H_g vibration shows 78% $l = 2$ stretch component (made with the help of τ parameter derivatives, depicted in Figure 5).

Thus, the radial nature of the lowest vibrations and the nice ordering with respect of l number of the spherical harmonics description is analytically noticed. A numerical experiment showed that the decoupled radial and tangential modes produce low frequencies close to those of radial A_g vibration. Even though the first mode is mainly radial, the 26% tangential mixture is crucial to achieve the lowest frequency. As corollary of actual discussion, we suggest promising further advances in conceiving a new type of force field explicitly based on the radial vs. tangential dichotomy (instead of the regular neighbour bond parameters expansions[5]). Here we confined ourselves to a quantitative modeling of A_g modes, the semiquantitative extrapolation on the H_g ones, pointing in addition that the T_{1u} case follows a similar qualitative principle.

$$q(2,z^2)_R \propto \sqrt{\frac{5}{16\pi}}(2z^2-x^2-y^2) \qquad\qquad q(2,x^2-y^2)_R \propto \sqrt{\frac{5}{16\pi}}(x^2-y^2)$$

$$q(2,z^2)_V \propto V_{z^2} \qquad\qquad q(2,x^2-y^2)_V \propto V_{x^2-y^2}$$
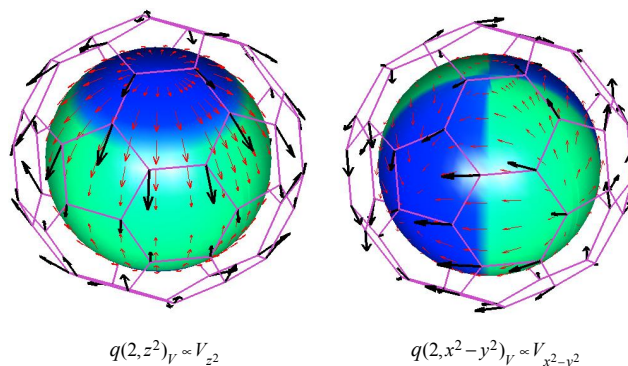
Figure 3 Selected members with $l=2$ parentage for radial (spherical harmonics, $Y_{20} \propto z^2$ and $Y_{22}{}^c \propto x^2$-y^2) and tangential (vector surface harmonics, V_{20} and $V_{22}{}^c$) components in the lowest H_g vibration. The colors on the inner sphere represent the sign (blue-positive, green-negative) of the selected spherical harmonics component. The length of arrows on the sphere is proportional with the magnitude of the Y or V functions. Their orientation depends on the Y sign and nodes. The radial or tangential displacement of the cluster atoms is proportional with the Y or V functions, respectively, at the atom polar coordinates.
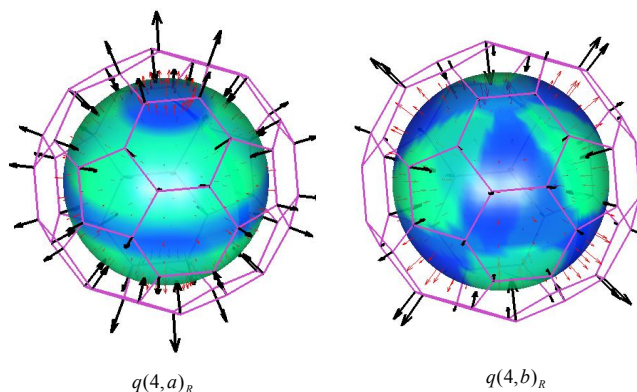

$$q(4,a)_R \qquad\qquad q(4,b)_R$$

Figure 4. Selected symmetry adapted components (a and b are arbitrary labels) of the radial mode with Y_{4m} definition, preponderantly forming the second H_g vibration. The colors and arrows on the sphere depicted inside denote the sign and magnitude of the spherical functions. The displacements of the C_{60} atoms parallel the spherical function at the given position.
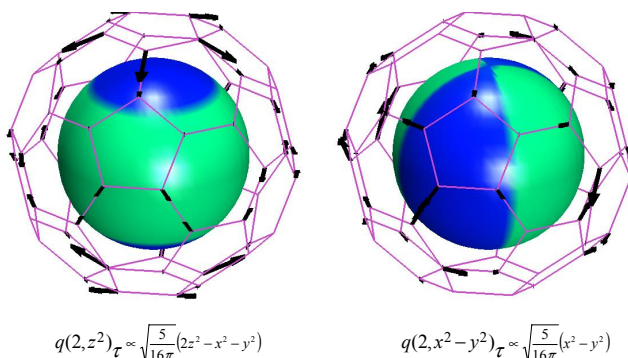

$$q(2,z^2)_\tau \propto \sqrt{\tfrac{5}{16\pi}}\left(2z^2-x^2-y^2\right) \qquad\qquad q(2,x^2-y^2)_\tau \propto \sqrt{\tfrac{5}{16\pi}}\left(x^2-y^2\right)$$

Figure 5. The bond stretch mode with Y_{20} and $Y_{22}{}^c$ type modulation of the tangential A_g function, mainly forming the fourth H_g vibration.

[1] a) N. V. Cohan, *Proc. Cambridge Philos. Soc.* **1958**, *54*, 28; b) P. W. Fowler, A. Ceulemans, *Molec. Phys.*, **1985**, *54*, 767; c) A. Y. Li, M. Z. Liao, *Int. J. Quantum Chem.* **2001**, *83*, 286-302.

[2] a) A. J. Stone, *Mol. Phys.* **1980**, *41*, 1339-1354; b) A. J. Stone, *Inorg. Chem.* **1981**, *20*, 563-571.

[3] a) D. M. P. Mingos, *Nature* **1990**, *345*, 113-114. b) D. M. P. Mingos, R. L. Johnston, *Struct. Bonding* **1987**, *68*, 29-87; c) A. Ceulemans, G. Mys, *Chem. Phys. Lett.* **1994**, *219*, 274-278.

[4] a) S. F. A. Kettle, E. Diana, R. Rossetti, P. L. Stanghellini *Inorg. Chem.* **1998**, *37,* 6502-6510; b) A. Ceulemans, P. W. Fowler, I. Vos *J. Chem. Phys.* 1994, 100, 5491-5500.

[5] a) Z. C. Wu, D. A. Jelski, T. F. George, Chem. Phys. Lett. 1987, 137, 291; b) R. A. Jishi, R. M. Mirie, M. S. Dresselhaus, Phys. Rev. B 1992, 45, 13685; c) A. Ceulemans, B. C. Titeca, L. F. Chibotaru, I. Vos, P. W. Fowler, J. Phys. Chem. A 2001, 105, 8284; d) I. D. Hands, J. L. Dunn C. A. Bates, J. Chem. Phys. 2004, 120, 6912- 6921.